DEVELOPMENT OF S-BAND PULSED KLYSTRON FOR PLS LINEAR ACCELERATOR*

S. J. Park#, S. H. Kim, Y. J. Park, K. R. Kim, S. D. Jang, Y. G. Son, J. S. Oh, Y. C. Kim, S. H. Nam, I. S. Ko, S. G. Baik (Pohang Accelerator Laboratory), M. H. Cho, and W. Namkung (Pohang University of Science and Technology), Pohang 790-784, Korea

Abstract

S-band pulsed klystron with > 65-MW output power has been developed in house, for use as backup rf sources in the PLS (Pohang Light Source) linear accelerator. Successful completion of the work is largely due to high-quality in-house resources including dedicated engineering experts, special facilities for klystron fabrication & processing, and infra-structures established during the PLS construction. Mechanical and electrical specifications conform to those of existing klystrons (Toshiba E3712), requiring no adjustments upon installation. Optimization or enhancement of operating characteristics can be done with the modification of cavity system, which would be a good further work. In this article, we will report on the whole design, fabrication, processing, and test procedures.

INTRODUCTION

The PLS is the third generation light source with the 2.5-GeV storage and the full energy (2.5 GeV) injector linac. The PLS linac is composed of 44 SLAC-style accelerating columns powered by twelve sets of 80-MW klystrons and modulators. Since their installation in 1992, many klystrons have exceeded 80,000 hours in their (heater) run times, and several ones have failed. Costs for klystron replacements have been and will be the significant fraction of the operating budgets. Due to this, there have been strong demands for having capabilities for the in-house fabrication of klystrons. It has been also expected that the capabilities also contribute to the future accelerator construction such as the linac-based 4th generation light source. In Table 1, we summarize design specifications of PLS linac klystrons together with achieved performances from developed one (details will be described in later sections).

Table 1: Major parameters of PLS linac klystrons.

	DESIGN	ACHIEVED
Frequency	2856 MHz	2856 MHz
Output Power (Nominal)	80 MW	80 MW @ 1 μs 65 MW @ 3 μs
Repetition Rate	Max. 60 Hz	Processed at 14 Hz
RF Pulse width	4 μs	3 μs
Efficiency	> 40 %	> 40 %
Gain	> 50 dB	> 50 dB

*Work supported by the MOST and the POSCO, Korea.
#smartguy@postech.ac.kr

In the Pohang Accelerator Laboratory (PAL), high-quality infra-structures including XHV cleaning shop, welding shop, 3-dimensional measuring facility have been established during the PLS construction. Along with these, we have also established special facilities for the klystron fabrication such as XHV baking station, UHV brazing furnaces, and cathode processing facility. Using these, we have already rebuilt one out of two failed klystrons [1] and it has been in service in the PLS linac for more than 1.5 years.

DESIGN WORK

Electron Gun

The design of the electron gun starts with considering the cathode loading. From this, we can determine the cathode size. Another important factor determining the cathode size is the electric field strength on electrode surfaces. In Pierce-type guns, the surface field is lowered with increased cathode size, but with some practical limitation. Too big cathode size will make the electron gun and hence the klystron unacceptably large. Also the bigger cathode results in higher convergent beam, and it becomes more difficult to control the trans-laminar flow in the beam edge. Systematic gun-design procedures can be referred from [1] & [2].

Although the overall design of the electrodes shapes in the Pierce gun can be done following the method in [2], practical design usually requires numerical simulations using computer code such as the EGUN. Fig. 1 shows the beam trajectories in the electron gun obtained from the EGUN simulation.

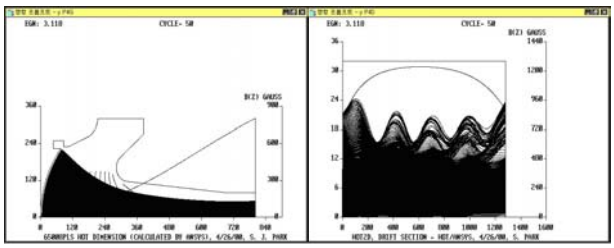

Figure 1: Beam trajectories inside (left) and downstream (right) of electron gun, obtained from EGUN simulations.

EGUN simulations are very useful in determining electrode shapes and key parameters including the perveance. But dimensions used in gun parts machining are different from those determined in the EGUN simulation, because the EGUN assumes the cathode is heated up to its operating temperature (~1000 °C), and dimensions with the hot cathode (hot condition) are

different from those with the cold one. This is significant in high-power guns with large cathodes. In order to estimate the amount of the thermal expansion in gun electrodes, we have used the ANSYS code. The coupled-mode (thermal-mechanical) analysis of the code can predict mechanical deformation due to thermal expansion, with given temperature distribution obtained from the prior thermal computation. Fig. 2 is the result of the ANSYS computation for the thermal expansion of the cathode assembly (= cathode + focus electrode + cathode stem). Since the anode is water-cooled, its thermal expansion was assumed negligible.

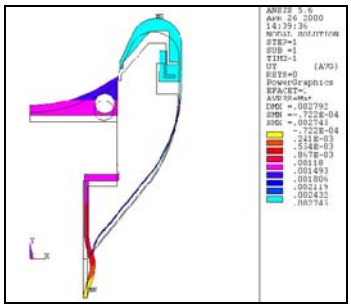

Figure 2: Axial (upward) expansion of cathode assembly when cathode is heated to 1000 °C, computed by ANSYS code. Deformed shape (shaded) is overlaid with original one. Maximum expansion was about 2.5 mm at focus electrode tip.

The calculated thermal expansion, ~2.5 mm was so large that it was expected to cause the perveance error > 10 % when one does not incorporate it into fabricating the gun. We have prepared a model cathode assembly, installed it in the cathode-processing furnace that is equipped with a quartz vacuum chamber and auxiliary instrumentations, and measured the thermal expansion. The tip of focus electrode was found to axially expand by 2.4 mm, which is in good agreement with the ANSYS computation [4].

Cavity System

Design of cavity system includes determination of inter-cavity distances, cavity resonant frequencies, coupling parameter (β) of input and output cavities, and other parameters such as drift tube diameter and cavity HOM frequencies. Successful design for high-power klystron requires computer codes that can fully consistently simulate the interaction between the beam and cavity fields. We have used the FCI (Field-Charge Interaction) code [5].

The coupler in the input cavity should be carefully designed to include the beam-loading effect. The matching condition with the beam-loading effect is to provide the detuning, δ and the coupling parameter β for the input cavity in the "cold condition" (i.e., without the beam), given by the following equations [6],

$$\delta = \frac{f_o - f}{f} = -\frac{R/Q}{2}\,\mathrm{Im}\left(\frac{1}{Z_b}\right) \qquad (1)$$

$$\beta = \mathrm{Re}(1 - R_c / Z_b) \qquad (2)$$

where, f_o = Resonant frequency of the input cavity,
f = Drive frequency to the input cavity,
R/Q = R/Q factor of the input cavity,
Z_b = Beam impedance,
R_c = Cavity impedance.

With numerical values, R/Q = 65, Q_o = 2000, the detuning parameter δ = 1.6 MHz. Since R_c = R/Q x Q_o = 130 □, β = 10.1.

Traditionally, the shape of the input coupler with the required β has been determined experimentally. The numerical calculation of the coupler geometry is now possible with the use of 3D codes, e.g., HFSS. The β is found by calculating the S_{11} and converting it to the VSWR (Voltage Standing Wave Ratio). In an over-coupled case, the β is simply the VSWR (Fig. 3). The accuracy of the β determined by this method heavily depends on the accuracy of the Q_o factor (i.e., the wall loss) of the cavity. The Q_o of a real cavity not only depend on the properties of cavity material but also on fabrication procedures such as cleaning method, brazing and bake-out processes. Numerical simulations with the HFSS or the SUPERFISH codes do not account for these effects. But, it is empirically known that the Q_o for a real cavity is at most half that predicted by simulation. Measured β after fabrication was 12.

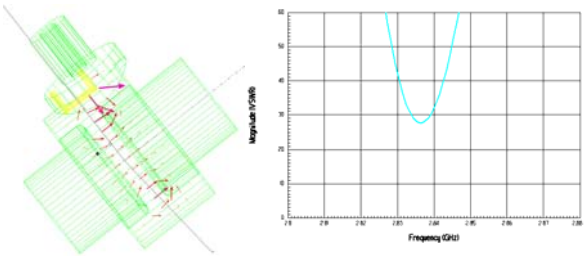

Figure 3: Design of input coupler using HFSS code. Shown are 3D modelling of the geometry (left) and plot of calculated VSWR versus frequency (right).

The optimum β of the output cavity is determined by the gap voltage that yields highly efficient beam-to-rf energy conversion in the output cavity. From the FCI simulations, we have found that optimum cavity voltage is obtained at its rms value of roughly the same as the beam voltage. Given this condition and typical the R/Q value for the S-band klystron (for our case, 85), the optimum β was about 200. Design of the output coupler by the use of HFSS is relatively easy, for the double coupler as used in the Toshiba E3712 klystron. This is because we can determine the β (or Q_L) by calculating the S_{21} for the two coupler waveguides and finding the 3-dB bandwidth. Again we have used Q_o = 2000 here.

FABRICATION

The gun anode and cavities were machined with the ultra-precision turning lathe (Nanoform600). With this, Ra values of 15.6 and 8 nm were achieved at the anode and cavity surfaces respectively. Machined parts were chemically cleaned followed by thorough pure-water rinsing. All parts were brazed in an UHV brazing furnace that was conditioned to provide high 10^{-8} Torr at 1000 ^{o}C. Stainless steel structures surrounding the cathode were vacuum brazed with pure copper (melting point = 1083 ^{o}C) as the filler metal. The pure copper showed excellent wetting and flowing on the stainless steel. Radiation heats from the side wall of the cathode were shielded by stacked (and dimpled) Molybdenum foils.

The cathode assembly was processed before integrating into the gun. For this we have used an UHV induction furnace with Molybdenum radiator (susceptor) between the induction coil and the cathode assembly. The cathode was slowly heated to the (brightness) temperature of 950 C_B with final ramping up to 1000 C_B. It took several days to complete the whole process. During this, the focus electrode was removed in order to prevent possible oxidation on its surface. The focus electrode was de-gassed using the UHV brazing furnace at 1000 ^{o}C for several hours.

In order to provide enough bandwidth for tuning the output cavity, E-bends, instead of easy-to-make E-corners, were used in double-output couplers. High-quality bending of waveguide was very difficult and we resorted to the machining by milling machine.

After all sub-assemblies were ready, the cathode assembly was pulled out from the induction furnace and mounted in the gun base-plate. We have used special jigs for the centre-line alignment of the cathode and the anode, and to adjust the gap distance between the latter and the focus electrode tips. The gun, cavities, and the collector were assembled by welding stainless-steel lips brazed at interfaces of each sub-assembly. After attaching a pumping tube (made of annealed copper tube) at the bottom of the gun, the whole klystron assembly was mounted on the baking station. With separate pumping for output windows, the inside and the outside of the klystron were pumped by a cryo and a diffusion pumps. The klystron was baked at 550 ^{o}C for 200 hours. There was heavy out-gassing of water molecules up to 150 ^{o}C. Later on, dominant de-gassing was by the Hydrogen gas. There were small and decreasing de-gassings of carbon mono- and di-oxides, especially when the cathode was turned at the final stage of the bake-out process.

After cool-down, the pinch-off was with small and momentary pressure jump at the 20-l/s ion pump attached to the (H-plane of) waveguide of one output coupler. Dressing was done with cooling pipes, water jackets, Lead shields, and the cathode heater transformer. The finished klystron was moved to the test-lab for aging processes.

PROCESSING

The klystron was processed to yield 80 MW at the rf pulse length of 1 μs. With increased rf pulse length up to 3 μs, it is stably generating > 65 MW. Rf power measurement for the 3-μs operation was done by the calorimetric method with the accuracy of < 1 % [7]. Performances of the klystron are summarized in Fig. 4. One problem observed as of now is non-catastrophic gun arcings (3-4 times a day at > 65 MW output, none at < 50 MW) which are believed to be caused by surface breakdowns on the vacuum side of the gun ceramic insulator. It would be possible to eliminate this by adopting better ceramic material. The klystron is waiting for its service in the PLS linear accelerator.

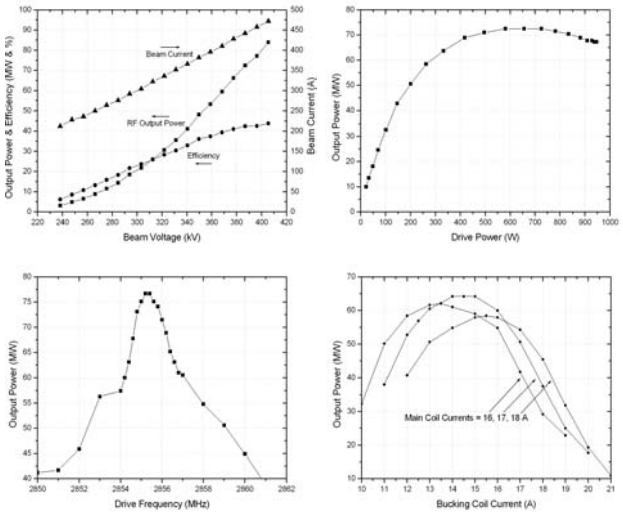

Figure 4: Performances of fabricated klystron: Rf output power and efficiency versus beam voltage (upper left), Transfer characteristics (upper right) – available rf input to the input cavity should include ~ 3-dB cable attenuation, Bandwidth characteristic (lower left), and Rf output power versus various combination of bucking and focus coil currents (lower right).

REFERENCES

[1] S. J. Park et al., Proc. of the 2000 KAPRA & KPS DPP Joint Workshop.

[2] J. Rodney and M. Vaughan, IEEE ED-28, pp. 37-41 (1981).

[3] R. Latham, *Electrical Breakdown in Vacuums*, Academic Press (1995).

[4] S. J. Park et al., Proc. of the LINAC2002, pp. 196-198 (2003).

[5] T. Shintake, NIM-A363, pp.82-89 (1995).

[6] B. E. Carlsten et al., IEEE ED-44, pp. 894-900 (1997).

[7] J. S. Oh et al., Bulletin of the Korean Physical Society, Vol 19, No. 2, Oct. 2001, p. 175.